Analysis of electron energy distribution function in a magnetically filtered complex plasma

M K Deka, H Bailung, and N C Adhikary†

Physical Sciences Division, Institute of Advanced Study in Science and Technology, Vigyan Path, Paschim Boragaon, Garchuk, Guwahati-781035, Assam, India

(Received 10 September 2012; revised manuscript received 6 December 2012)

The electron energy distribution function (EEDF) for a magnetically filtered dusty plasma is studied in a dusty double plasma device where the electron energy can be varied from 0.15 eV to $\sim$ 2.8 eV and plasma density from 10^6 cm^{-3} to 10^9 cm^{-3}. The characteristics of EEDF for these ranges of plasma parameters are investigated in a pristine plasma as well as in a dusty plasma. The results show that in the presence of dust, there is a drastic modification in EEDF patterns in a plasma with higher electron temperature and density than those in a low temperature and low density plasma produced by the magnetic filter.

Keywords: dusty plasma, magnetic filter, electron energy distribution function

PACS: 52.25.–b, 52.27.Lw, 52.70.–m, 52.20.–j **DOI:** 10.1088/1674-1056/22/4/045201

1. Introduction

The control of plasma parameters such as electron temperature, electron density, sheath potential, and electron energy distribution function (EEDF) in a weakly ionized plasma is of much importance in many plasma-based applications.[1] Since these plasma parameters are essential to study the dependences of different particle elementary processes and plasma collective phenomena in weakly ionized plasmas.[2] In some recent experimental works, different techniques have been reported to optimize those plasma parameters using different plasma devices.[3–7] In addition, the EEDF is closely related to the rates of major changes in elementary processes, and it determines the stability as well as the dynamic properties of plasma.[8–12] Therefore, the control of EEDF is one of the most important challenges in the application of chemically active plasmas in plasma processing reactors.[13,14] In general, EEDF is calculated from the double derivative of the experimentally measured Langmuir probe *I*–*V* characteristics[15] but some authors have also reported on a few other models to estimate EEDF in a plasma in different ways.[16–19]

It is well understood that the presence of micron-sized charged dust particles in plasma drastically changes the plasma parameters and sheath potentials, and also affects the collective processes in such plasma systems.[20,21] Denysenkoa *et al*.[22] and Ostrikov *et al*.[23] studied the properties of EEDF in the presence of dust particles in a plasma and they concluded that a typical Druyvesteyn-like EEDF in a pristine plasma may become Maxwellian one in the presence of the sufficient number of dust particles. For non-equilibrium plasmas, such as low pressure discharge plasma, the electrons are in equilibrium neither with other plasma components, nor with the electron ensemble itself.[15] This means that the EEDF of such a plasma is non-Maxwellian, and as a result the plasma modeling is much more complicated.[24] Therefore, to characterize the plasma, it is important to know the energy distribution of the electrons, which is directly related to not only the chemistry of the electronic kinetic processes within bulk plasma but also the electron density and temperature.[25,26]

Again, the role of ambient plasma condition (density, temperature, etc.) in dust charging processes has been studied by many researchers based on the OML approximation.[27,28] Kaushik *et al*.[28] studied the effect of electron temperature on dust charge and they observed a reduction in dust charge with the decrease in electron temperature even after increasing plasma density. However, this peculiar observation should be well understood, because although the electron temperature is a determinative factor in determining the dust charge but the role of plasma density cannot be neglected as indicated in earlier reports.[29–31] Though there is much research work on EEDF, which has reported from time to time, to our knowledge no experimental evidence is available which shows the effect of dust on EEDF in a plasma at the most fundamental level. Hence, in this paper, based on the techniques for the determination of EEDF from the double derivative of Langmuir probe *I*–*V* characteristics,[15] different important features of EEDF in a dusty plasma are presented. Finally, the measured EEDFs are compared with the existing theoretical one.

2. Experimental procedure

The experiment is performed in a dusty double plasma device and the schematic diagram is shown in Fig. 1. The device is divided into two sections, namely the source and the

†Corresponding author. E-mail: nirab_iasst@yahoo.com

© 2013 Chinese Physical Society and IOP Publishing Ltd

target by a magnetic filter made by an arrangement of permanent magnets. The magnetic filter is composed of 5 permanent magnets that are similar to those used for surface plasma confinement and are fixed at 3.4 cm apart from each other with opposite pole orientations. The maximum pole field strength of each magnet (1.8 cm in thickness, 1.0 cm in breadth) is 0.07 T. The details of the filter configuration (field mapping, etc.) have already been reported by Bailung *et al*.[29]

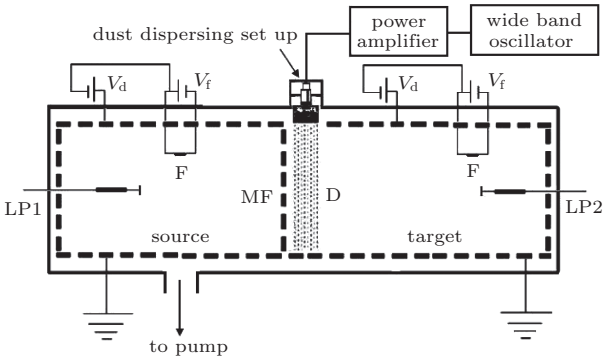


Fig. 1. Schematic diagram of the experimental device, F-filament, V_d-discharge voltage, V_f-filament heating voltage, MF-magnetic filter, D-dust column, $LP_{1,2}$-Langmuir probe.

The chamber is evacuated down to 2.0×10^{-4} Pa using an oil diffusion pump backed by a rotary pump. The experimental observations are recorded at different working pressures (5.3×10^{-2} Pa to 1.2×10^{-1} Pa)) by injecting argon gas at a desired partial pressure under continuous pumping. Plasma can be produced both in the source section and in the target section independently by filament glow dc discharge. The discharge voltage is kept fixed at 60 V and discharge current is varied within a range from 50 mA to 450 mA.

Now, to produce dusty plasma, a sufficient number of dust particles is dispersed from the dust dispersing setup mounted at the top of the target section, and dust density can be varied from $\sim10^3$ cm^{-3} to $\sim10^4$ cm^{-3}. The edge of the dust column is placed at a distance about 6 cm from the magnetic filter surface to avoid the effect of magnetic field. Plasma parameters such as electron density, electron temperature, etc. are measured in the target section as well as in the source section using two planner Langmuir probes each with 6 mm in diameter. The average charge quantity acquired by a dust grain is calculated from the reduction in the electron density using the modified charge neutrality condition for such a plasma. To produce a low density and low temperature plasma in target section, discharge takes place only in the source section. And the plasma is allowed to diffuse from source to target section through the magnetic filter. The high energetic electrons in the source plasma are then captured or reflected by the magnetic field lines and only low energy electrons are allowed to pass through the magnetic filter towards target section.[29] However, the target section is also equipped with discharge generating system, so plasma is produced in the target section also whenever necessary to obtain higher electron temperature and density there.

3. Results and discussion

The EEDF is analyzed based on the technique of determining electron energy distribution function for Maxwellian as well as for non-Maxwellian but isotropic plasma from the double derivative of *I*–*V* characteristics.[15] In the presence of discharge on both sides of the double plasma device, the EEDF is measured in the target section for three different partial pressures of argon. It is seen from Fig. 2 that as the working pressure is increased from 5.3×10^{-2} Pa to 1.2×10^{-1} Pa, the EEDF behaves like a typical Druyvesteyn type because of the depletion in the high energy tail of the EEDF due to more collisions with the increase of the neutral particle density which often exists in such a type of plasma environment.[4] The electron temperature (T_e) shows a decrease in its value from 1.8 eV to 1.1 eV while the electron density (n_e) increases from 1.5×10^9 cm^{-3} to 6.5×10^9 cm^{-3} as working pressure is increased from 5.3×10^{-2} Pa to 1.2×10^{-1} Pa.

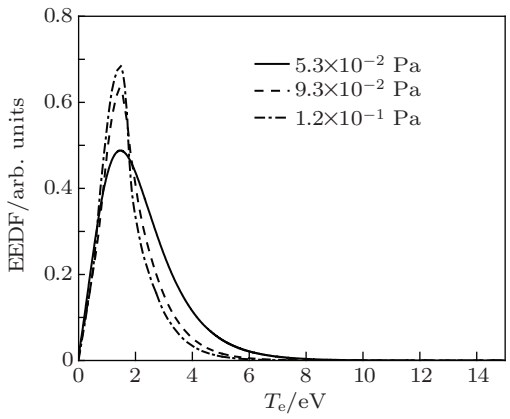


Fig. 2. EEDF patterns at different values of partial pressure (P) of argon. The solid line represents the data for $P = 5.3\times10^{-2}$ Pa, dash line for $P = 9.3\times10^{-2}$ Pa, and the dashed-dot line for $P = 1.2\times10^{-1}$ Pa.

Now to carry out the EEDF study in the presence of dust particles the working pressure is kept at 9.3×10^{-2} Pa. And then dust particles are introduced into the plasma with different concentrations and the results are summarized as follows. As described above, in this pressure range the electron energy distribution function behaves like a typical Druyvesteyn type in the absence of dust particles. Typical *I*–*V* characteristics in the presence of different dust densities are shown in Fig. 3. The corresponding discharge voltage is fixed at 60 V and discharge current is kept at 150 mA both in the source section and in the target section. The EEDF in the presence of dust particles is estimated from this set of *I*–*V* plots. As seen from the figure, as the dust density is increased from $n_d = 0$ to 3.98×10^4 cm^{-3} the average T_e is increased from 1.47 eV

to 2.6 eV and accordingly a depletion in n_e is observed from 1.57×10^9 cm^{-3} to 0.65×10^9 cm^{-3}. This is due to the fact that as the dust particles are introduced into the system low energy electrons are captured by dust grains, and hence the average energy of the electrons increases and density decreases. This experiment is repeated for different discharge currents (50 mA to 250 mA) with the discharge voltage kept fixed, and similar trends of results are observed.

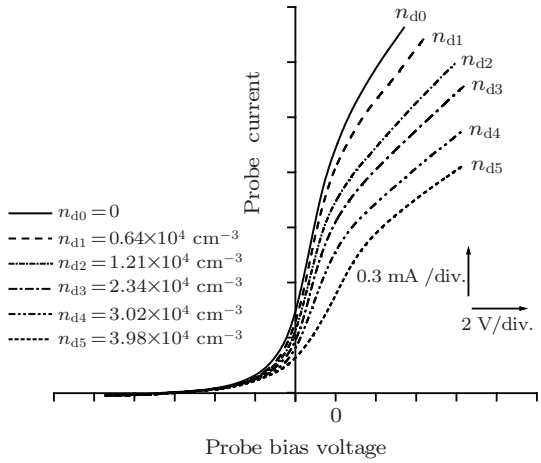


Fig. 3. Typical Langmuir probe *I–V* characteristics recorded at different dust particle densities. The solid line represents the data for the no dust condition, dashed line for n_{d1}, short-dash–dot line for n_{d2}, dash–dot line for n_{d3}, dash–dot–dot line for n_{d4}, and short-dash line for n_{d5}.

Now, the EEDF patterns for different dust densities are shown in Figs. 4(a) and 4(b). In these figures the solid curve represents the theoretical Maxwellian EEDF, the dotted curve represents the theoretical Druyvesteyn EEDF whereas the solid square point represents the experimentally measured EEDF pattern. The theoretical curves have been obtained from the well-known expressions for Maxwellian and Druyvesteyn distribution.[32] As seen from Fig. 4(a), for a small dust density ($n_d = 0.64\times10^4$ cm^{-3}) the EEDF retains its typical Druyvesteyn shape even after introduction of dust particles. But as the dust density is increased from $n_d = 0.64\times10^4$ cm^{-3} to $n_d = 3.02\times10^4$ cm^{-3} the distribution starts to become typical Maxwellian type as shown in Fig. 4(b). A similar trend is noticed as dust density further increases to $n_d = 3.98\times10^4$ cm^{-3}. The reason behind this transition is that as dust particles are introduced into the system low energy electrons are captured by dust grains and thus the average energy of the plasma electrons increases and thus the EEDF shows an increase in the high energy tail and an overall depletion of the electron population. The Maxwellization of the EEDF at high dust densities can also be attributed to electron–dust collisions. These inelastic electron–dust collisions often result in low energy electron capture by the dusts since electrons are collected by the dust grains. Due to the enhanced loss to the dust grains, at relatively high dust density, electron density decreases dramatically with dust density increasing. With the increase of the total electron loss (to the dust grains), the system then self-organizes to maintain a balance between production and loss of electrons by increasing the number of electrons in the high-energy tail of the EEDF. That is, inelastic electron–dust collisions cause the electron EEDF to become Maxwellian. This Maxwellization of EEDF has been studied extensively by Ostrikov *et al.*[23] from the theoretical point of view for different dust densities and dust particle sizes. They also reported that not only with dust density increasing but also with dust particle radius (size) augmenting, the Maxwellization of EEDF can take place. However to our knowledge till now no experimental evidence has been reported. Our observation closely follows their numerical results.

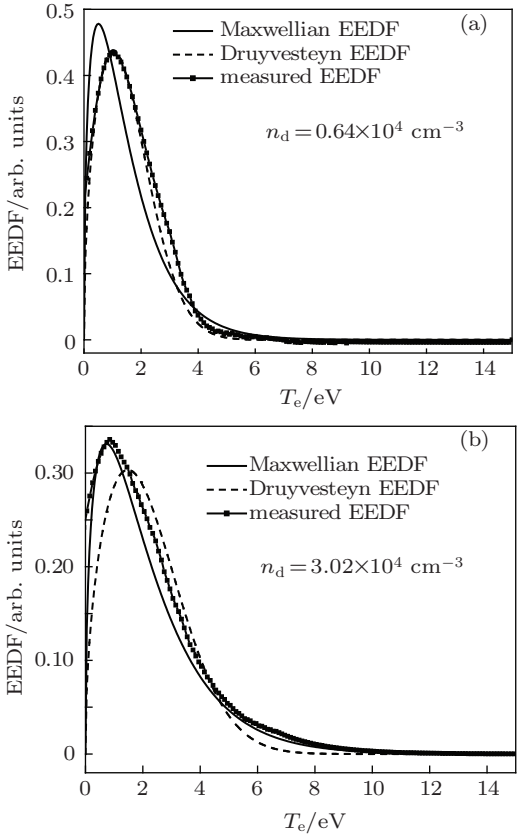


Fig. 4. EEDF patterns (a) for $n_d \sim 0.64\times10^4$ cm^{-3} and partial pressures of argon is kept fixed at 9.3×10^{-2} Pa and (b) for $n_d \sim 3.02\times10^4$ cm^{-3}. The solid line represents the Maxwellian EEDF, the dashed line represents the Druyvesteyn EEDF, while the solid square points represent the corresponding experimental points.

Next, to study the EEDF in a low temperature and low density plasma, the plasma in the plasma device is produced only in the source section and is allowed to diffuse towards target section through the magnetic filter placed between the source and target.[29] The discharge current (I_d) in the source is varied from 50 mA to 450 mA with the discharge voltage kept fixed at 60 V. The n_e and T_e profile in source are shown in Fig. 5 (lower panel). It is observed that in the source plasma, the density as well as temperature increases up to a certain discharge current (250 mA). However, beyond 250 mA, even

after increasing discharge current, the change in electron temperature is not much prominent but density increases reasonably.

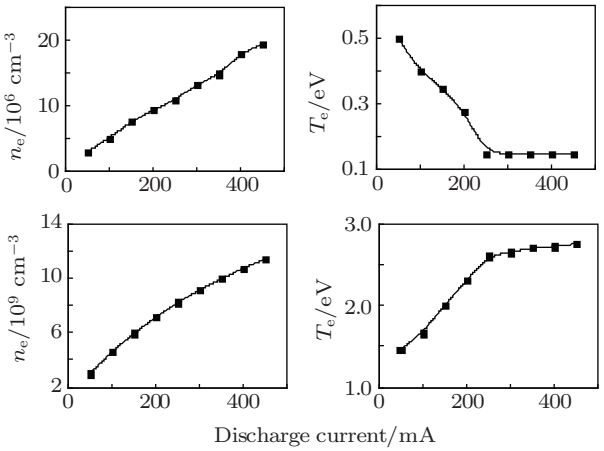


Fig. 5. (upper panel) electron density and electron temperature profile in target plasma for source discharge current ranging from 50 mA to 450 mA. (Lower panel) electron density and electron temperature profile in source plasma for the same range of discharge current.

On the other hand, the T_e and n_e profile in the target section represented in Fig. 5 (upper panel) show that the plasma in the target section contains low density and low energetic electrons. But the T_e value arrives at a saturation level ~ 0.15 eV beyond the source discharge current 250 mA, while n_e value increases with the increase of source discharge current. Now, EEDFs of the filtered plasma are studied for different source discharge currents and it is observed that the EEDF follows a typical Maxwellian type as shown in Fig. 6. The EEDFs for typical source discharge current from 250 mA to 450 mA shown in Fig. 6 signify the fact that even after increasing discharge current no substantial change in average T_e is observed but plasma density increases. The experiments are repeated for different argon partial pressures starting from 5.3×10^{-2} Pa to 1.2×10^{-1} Pa but no significant change in the electron energy distribution is observed. The density in the target section rises with source discharge current increasing, which is due to more charged particle diffusion from the source since the leakage width for charged particles across CUSP (the filter is of CUSP geometry) increases with discharge current increasing.[33] The decrease of T_e in the target section with the increase of I_d in the source section as well as the saturation of T_e beyond a certain limit of source discharge current (250 mA) may be due to the effect of electron diffusion through a magnetic filer. The expression for the electron diffusion coefficient across magnetic field is $D_\perp = \kappa_B T_e \nu/(\omega^2+\nu^2)$, where κ_B is the Boltzmann's constant, $\nu = 2.91\times10^{-6}\ln\Lambda n_e T_e^{-3/2}$ is the total electron collision frequency and the electron cyclotron frequency under the influence of magnetic field B is $\omega = eB/m_e$ with m_e being the mass of electron and $\ln\Lambda$ being the Coulomb logarithm.[34] From this expression two clear regimes can be identified which are as follows. In the low magnetic field limit, when $\omega < \nu$ and $D_{\perp l} = \kappa_B T_e^{5/2}/(2.91\times10^{-6}\ln\Lambda m_e n_e)$. But in the higher magnetic field limit, when $\omega \geq \nu$, the plasma electrons are magnetized and accordingly we can have $D_{\perp h} = 2.91\times10^{-6}\ln\Lambda\,\kappa_B T_e^{-1/2} n_e m_e/e^2B^2$. In our experimental condition we have $\nu \sim 10^5$/sec and $\omega \sim 10^9$/sec, therefore in the present condition electrons are magnetized and accordingly only relatively cold electrons have high diffusion rate across the magnetic filter.

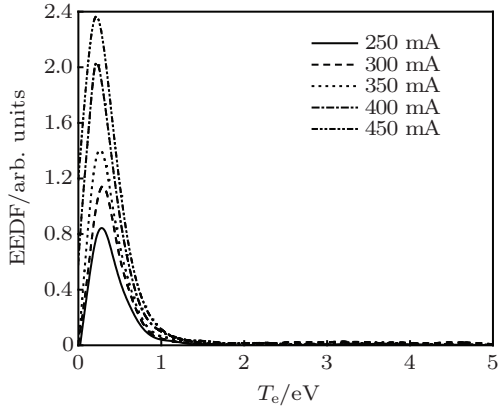


Fig. 6. EEDF patterns in target plasma for source discharge current varying from 250 mA to 450 mA. The electron temperature is 0.15 eV and electron density varies from 1.31×10^7 cm^{-3} to 1.93×10^4 cm^{-3}. The solid line represents the EEDF in target plasma for source I_d = 250 mA, dashed line for I_d = 300 mA, dotted line for I_d = 350 mA, dash–dot line for I_d = 400 mA, and the dash–dot–dot line for I_d = 450 mA.

On the other hand, since the diffusion coefficient is inversely proportional to the square root of T_e and the target plasma is totally dependant on source plasma, as T_e in source plasma increases with discharge current increasing, a greater number of low energy electrons diffuse from the source. But after a certain discharge current it is seen from Fig. 5 (lower panel) that the T_e value tends to be saturated and hence the same behavior is reflected in target also. Since all available electrons in the target chamber are low energetic, they cannot make effective ionization and hence plasma in the target chamber is of low density also. Qualitatively, this can also be attributed to the fact that the electron-neutral collisional cross section weakly depends on temperature (kinetic energy) and with temperature decreasing it rises slowly due to the prolongation of the interaction time.[35] Again, mean free path is inversely proportional to the collision cross section, thus with the increase of collision cross section the mean free path decreases and hence the electron cannot transfer its energy to the neutral atom further. Therefore, the saturation in T_e can be observed at a certain density in the target section. However, the detail of heat transport across a magnetic filter is beyond the scope of this paper but work in this direction is underway and will be communicated elsewhere.

After that, the EEDF in the presence of dust is investigated. The typical I–V characteristics in target plasma for a

source discharge current 450 mA at different dust densities are shown in Fig. 7(a). It is seen from the figure that even after introducing dust particles into the plasma, T_e remains unchanged and only plasma density decreases. The reasons are obvious: since the target plasma contains only low temperature electrons after introduction of dust grains, only plasma density is reduced due to loss in charging of dust grains but the average T_e value remains unchanged. This may be due to the fact that at this condition almost all the electrons have the same temperature. This can also be seen from the EEDF patterns shown in Fig. 7(b).

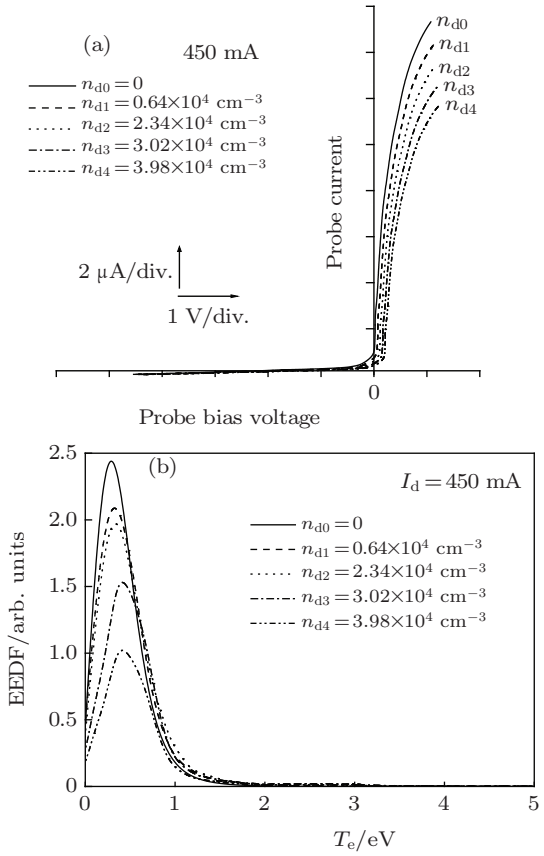


Fig. 7. Typical Langmuir probe *I–V* characteristics (a) and typical EEDF patterns (b) recorded at different dust densities in target plasma for a source discharge current 450 mA. The solid line represents the results obtained in no dust condition, dashed line represents results obtained at $n_{d1} = 0.64 \times 10^4$ cm^{-3}, dotted line at $n_{d2} = 2.34 \times 10^4$ cm^{-3}, dash–dot line at $n_{d3} = 3.02 \times 10^4$ cm^{-3}, and the dash–dot–dot line at $n_{d4} = 3.98 \times 10^4$ cm^{-3}.

Figure 8(a) shows the variations of average charge quantity acquired by the dust grains with dust particle density at different values of T_e when both source and target plasma discharge are on. The average charge quantity acquired by a dust grain is calculated from the reduction in the plasma density using the modified charge neutrality condition for such a plasma.[36] As seen from the figure, it is clear that the dust density is kept constant (at 0.64×10^4) as discharge current is increased from 50 mA to 250 mA. In this limit of I_d, the electron temperature T_e is increased from 1.47 eV to 2.6 eV, plasma density is increased from 1.57×10^9 cm^{-3} to 2.31×10^9 cm^{-3} and the calculated average dust charge quantity is found to increase from $2.81\times10^4 e$ to $4.53\times10^4 e$. The same observation is also found for other dust densities.

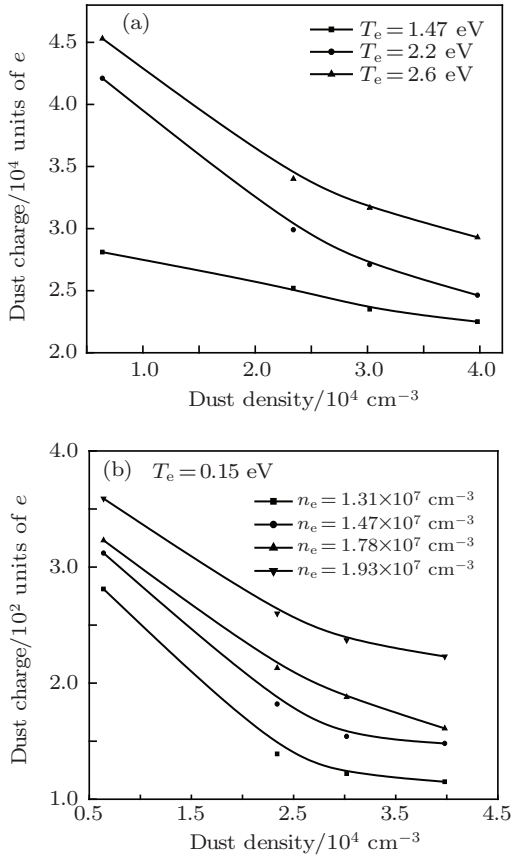


Fig. 8. Variations of measured dust particle charge quantity with dust particle density (a) for electron temperatures ranging from 1.47 eV to 2.6 eV and (b) for electron temperature 0.15 eV, electron densities from 1.31×10^7 cm^{-3} to 1.93×10^7 cm^{-3}, and source I_d 450 mA.

Again, this set of experiments is also performed in the case of magnetic filter plasma. We try to observe the dust charging process for the source discharge current (300 mA–450 mA). In this range of discharge current, plasma across magnetic filter typically exhibits only an enhancement in the value of n_e. The interesting phenomenon is observed here in this case: an increase in dust charge quantity is observed even if at constant plasma temperature, but with the increase of plasma density. The results are summarized in Fig. 8(b). It is observed that at constant T_e (~ 0.15 eV) and with plasma density increasing from 1.31×10^7 cm^{-3} to 1.93×10^7 cm^{-3} (percentage of increase 47%) the dust charge quantity increases from $2.81\times10^2 e$ to $3.59\times10^2 e$ (percentage of increase 27.7%). However, for plasma with higher T_e (1.47 eV or 2 eV), the plasma density increases at almost the same increase rate ($\sim 47\%$), the increase in the average dust charge quantity is measured to be around 61%. Therefore, for the same rate of change in plasma density, higher increase rate of dust charge quantity is observed in a higher T_e (~ 2.6 eV) plasma than in

a low T_e (0.15 eV) plasma. The same trends are also noticed in other dust densities.

4. Conclusion

In the present work the effects of negatively charged dust grains on the EEDFs for different plasma densities ranging from 10^6 cm^{-3} to 10^9 cm^{-3} and plasma temperatures from 0.15 eV to 2.8 eV are investigated. It is observed that typical Druyvesteyn-like EEDF in a pristine plasma may behave like Maxwellian type in the presence of sufficient concentration of dust grains. Also, it is observed that dust grains are unable to change the characteristics of EEDF in a low temperature (0.15 eV) and low density (10^6 cm^{-3}) plasma. We also demonstrate the crucial role of T_e in dust charging by measuring the values of dust particle charge quantity in a wide range of T_e (0.15 eV to 2.8 eV) at different plasma densities. The results show that an increased rate of plasma density has practically less effect on dust particle charge quantity than the increase rate of plasma temperature.

References

[1] Samukawa S 1994 *Jpn. J. Appl. Phys.* **33** 2133
[2] Kato K, Iizuka S and Sato N 1994 *Appl. Phys. Lett.* **65** 816
[3] Huang X J, Xin Y, Zhang J and Ning Z Y 2009 *Chin. Phys. Lett.* **26** 055202
[4] Li G, Zhang Y, Xu Y J, Lin B, Li Y T and Zhu J Q 2009 *Chin. Phys. Lett.* **26** 105202
[5] Ding Q Y, Zhang S B and Wang J G 2011 *Chin. Phys. Lett.* **28** 053202
[6] Wang D Y, Ma J X, Li Y R and Zhang W G 2009 *Acta Phys. Sin.* **58** 8432 (in Chinese)
[7] Liu X M, Song Y H and Wang Y N 2011 *Chin. Phys. B* **20** 065205
[8] Denysenko I, Yu M Y, Ostrikov K, Azarenkov N A and Stenflo L 2004 *Phys. Plasmas* **11** 4959
[9] Lieberman M A and Lichtenberg A J 1994 *Principles of Plasma Discharges and Materials Processing* (New York: Wiley) p. 711
[10] Godyak V A, Piejak R B and Alexandrovich B M 1992 *Phys. Rev. Lett.* **68** 40
[11] Godyak V A, Piejak R B and Alexandrovich B M 1995 *Plasma Sources Sci. Technol.* **4** 332
[12] Smolyakov A I, Godyak V A and Tyshetskiy Y 2001 *Phys. Plasmas* **8** 3857
[13] Sugai H, Ghanashev I, Hosokawa M, Misuno K, Nakamura K, Toyoda H and Yamauchi K 2001 *Plasma Sources Sci. Technol.* **10** 378
[14] Xu S, Ostrikov K, Li Y N, Tsakadze E and Jones I R 2001 *Phys. Plasmas* **8** 2549
[15] Druyvesteyn M J and Penning F M 1940 *Rev. Mod. Phys.* **12** 87
[16] Shi F, Zhang L L and Wang D Z 2009 *Chin. Phys. B* **18** 1177
[17] Sun J Z, Li X T, Bai J and Wang D Z 2012 *Chin. Phys. B* **21** 055205
[18] Li W, Chen J F and Wang T 2009 *Chin. Phys. B* **18** 2441
[19] Lin K X, Lin X Y, Chi L F, Yu C Y, Yao R H and Yu Y P 2009 *Chin. Phys. B* **18** 198
[20] Shukla P K 2001 *Phys. Plasmas* **8** 1791
[21] Wang J, Liu G, Yao L M and Duan X R 2012 *Acta Phys. Sin.* **61** 075205 (in Chinese)
[22] Denysenko I, M Y Yu, Ostrikov K and Smolyakov A 2004 *Phys. Rev. E* **70** 046403
[23] Ostrikov K, Denysenko I, Yu M Y and Xu S 2004 *J. Plasma Phys.* **71** part 2, 1
[24] Gudmundsson J T 2001 *Plasma Sources Sci. Technol.* **10** 76
[25] Bibinov N K, Kokh D B, Kolokolov N B, Kostenko V A, Meyer D, Vinogradov I P and Wiesemann K 1998 *Plasma Sources Sci. Technol.* **7** 298
[26] Godyak V A, Piejak R B and Alexandrovich B M 1995 *Plasma Sources Sci. Technol.* **4** 332
[27] Chakraborty M, Kausik S S, Saikia B K, Kakati M and Bujarbarua S 2003 *Phys. Plasmas* **10** 2
[28] Kausik S S, Chakraborty M and Saikia B K 2007 *Phys. Plasmas* **14** 024502
[29] Bailung H, Deka M K, Adhikary N C and Nakamura Y 2010 *Plasma Sources Sci. Technol.* **19** 055005
[30] de Angelis U and Forlani A 1998 *Phys. Plasmas* **5** 3068
[31] Shukla P K and Mamun A A 2002 *Introduction to Dusty Plasma Physics* (Bristol: Institute of Physics Publishing) p. 51
[32] Grill A 1994 *Cold Plasma in Materials Fabrication: From Fundamentals to Applications* (New York: IEEE Press) p. 9
[33] Anukaliani A and Selvarajan V 2001 *Eur. Phys. J. AP* **15** 199
[34] Holmes A J T 1982 *Rev. Sci. Instrum.* **53** 1517
[35] Franz G 2009 *Low Pressure Plasmas and Microstructuring Technology* (Berlin/Heidelberg: Springer-Verlag) p. 7
[36] Adhikary N C, Deka M K and Bailung H 2009 *Phys. Plasmas* **16** 063701